Supporting information for

3d Transition Metal and Nitrogen Co-Doped Graphene: First-principles Study of Electronic Structure and Optical Properties

Qingwei Zhang[a], Yanping Chen[b], Maoqin Wang[a], Yunhua Lu[a,*], Feng Zhang[b,*], Chao Zhang[c], Junan Zhang[a]

[a] School of Artificial Intelligence, Chongqing University of Technology, Chongqing 401135, China

[b] School of Physics and New Energy, Chongqing University of Technology, Chongqing 400054, China

[c] School of Chemical Engineering, Qinghai University, Xining 810016, China

Captions

1. Method

Equation S1. $E_b = E_{M-G} - (E_{V-G} + E_i)$

Equation S2. $\varepsilon(\omega) = \varepsilon_1(\omega) + i\varepsilon_2(\omega)$

Equation S3. $\varepsilon_2(q \to 0, \omega) = \frac{2e^2\pi}{V\varepsilon_0}\sum_{cvk}\left|\left\langle \psi_{\mathrm{k}}^{\mathrm{c}} \middle| \vec{u}\cdot\vec{r} \middle| \psi_k^v \right\rangle\right|^2 \delta(E_k^c - E_k^v - \omega)$

Equation S4. $\varepsilon_1(\omega) = \mathrm{Re}\left[\varepsilon(q \to 0, \omega) = 1 + \frac{2}{\pi}P\int_0^\infty \frac{d\omega' \varepsilon_2(\omega')\omega'}{\omega'^2 - \omega^2 + i\eta}\right]$

Equation S5. $\tilde{U} = n(\omega) + ik(\omega)$

Equation S6. $n(\omega) = \left(\frac{\sqrt{\varepsilon_1(\omega)^2 + \varepsilon_2(\omega)^2} + \varepsilon_1(\omega)}{2}\right)^{\frac{1}{2}}$

Equation S7. $k(\omega) = \left(\frac{\sqrt{\varepsilon_1(\omega)^2 + \varepsilon_2(\omega)^2} - \varepsilon_1(\omega)}{2}\right)^{\frac{1}{2}}$

Equation S8. $R(\omega) = \frac{(n-1)^2 + k^2}{(n+1)^2 + k^2} = \left(\frac{1 - \sqrt{\varepsilon(\omega)}}{1 + \sqrt{\varepsilon(\omega)}}\right)^2$

Equation S9. $\alpha(\omega) = \frac{2k(\omega)}{c\mathrm{h}} = \frac{\varepsilon_2(\omega)}{nc\mathrm{h}}$

2. Results and Discussion

2.1 Phonon dispersion analysis

Figure S1. The phonon spectra of (a) monolayer graphene and (b) CoNG are presented.

2.2 Band structure

Figure S2. The electronic band structure and density of states of (a)-(b) monolayer graphene and (c)-(d) N-doped graphene are presented.

2.3 Density of states

Figure S3. Density of states of C 2s in each doped system

2.4 Charge transfer mechanisms

Figure S4. (a-d) Charge difference density and Mulliken diagrams of Ti, V, Cr, and Cu doped elements.

2.5 CoNxG System

Table S1. shows the binding energy (E_b) of CoN$_x$G, the height h(Å) of Co atoms from the graphene plane, and the optimized bond lengths $l_{C\text{-}Co}$(Å) and $l_{N\text{-}Co}$(Å) after geometric structure optimization.

Figure S5. Phonon spectrum of CoN$_4$G.

1. Method

In this work, the electronic and optical properties of 3d transition metals co-doped with nitrogen atoms are investigated, and all calculations are based on first-principles density functional theory (DFT)[48] and implemented using the CASTEP module in Material Studio[49]. Our work is based on generalized gradient approximation (GGA) to exchange correlation energies with PBE functionalization, and Ultrasoft pseudopotential was used to calculate nucleus-electron interactions. To describe van der Waals interactions in layered materials, a DFT-D correction of Grimme remote dispersion correction was used[50].The cut-off energy was set to 600 eV, and the smearing width was set to 0.2 eV. The self-consistent field (SCF) tolerance was set to 1×10^{-6} eV/atom, and the convergence of energy, maximum force, maximum displacement were 1×10^{-5} eV/atom, 0.01 eV/Å and 0.001 Å, respectively. The Monkhorst-Pack method was used to sample the Brillouin zone, forming a uniform k-point mesh in reciprocal space, with a 6×6×1 k-point grid selected. All systems have spin polarization turned on. In addition, a vacuum layer thickness of 20 Å was used to mitigate interlayer interactions. In this paper, nitrogen atoms and transition metal atoms are selected as dopants to replace the carbon atoms in a periodic model slab of 4×4 supercell size.

Based on the stable structure of the original graphene, the binding energy (E_b) of doped graphene is expressed by the following formula:

$$E_b = E_{M-G} - (E_{V-G} + E_i) \tag{S1}$$

Here, E_{M-G} , E_{V-G} , and E_i represent the total energy of doped graphene, the energy of vacancy defective graphene, and the energy of doped atoms, respectively. A negative energy value indicates that the structure is stable after doping, and the larger the absolute value, the more stable the structure[51].

For any system, the evaluation of optical properties relies on a frequency-dependent complex dielectric constant:

$$\varepsilon(\omega) = \varepsilon_1(\omega) + i\varepsilon_2(\omega) \tag{S2}$$

The imaginary part $\varepsilon_2(\omega)$ of the dielectric function can be calculated using the linear response function:

$$\varepsilon_2(q \to 0, \omega) = \frac{2e^2\pi}{V\varepsilon_0}\sum_{cvk}\left|\left\langle \psi_{\mathrm{k}}^{\mathrm{c}} \middle| \vec{u}\cdot\vec{r} \middle| \psi_k^v \right\rangle\right|^2 \delta(E_k^c - E_k^v - \omega) \tag{S3}$$

where ω, ε_0, and V represent the frequency, vacuum capacitance, and unit cell volume of electromagnetic (EM) radiation, respectively. $\vec{u}$ and $\vec{r}$ represent the polarization vector and position vector of the incident electromagnetic field, respectively. ψ_k^c and ψ_k^v represent the wave functions of the conduction and valence bands, respectively. The real part ε_1 is transformed from the imaginary part ε_2 by the Kramers-Kronig dispersion relationship:

$$\varepsilon_1(\omega) = \mathrm{Re}\left[\varepsilon(q \to 0, \omega) = 1 + \frac{2}{\pi}P\int_0^\infty \frac{d\omega'\varepsilon_2(\omega')\omega'}{\omega'^2 - \omega^2 + i\eta}\right] \tag{S4}$$

where P represents the Cauchy value. This technique has been well explained in the references[52].

The complex index of the system is given by the following equation:

$$\tilde{U} = n(\omega) + ik(\omega) \tag{S5}$$

Where,

$$n(\omega)=\left(\frac{\sqrt{\varepsilon_1(\omega)^2+\varepsilon_2(\omega)^2}+\varepsilon_1(\omega)}{2}\right)^{\frac{1}{2}} \tag{S6}$$

$$k(\omega)=\left(\frac{\sqrt{\varepsilon_1(\omega)^2+\varepsilon_2(\omega)^2}-\varepsilon_1(\omega)}{2}\right)^{\frac{1}{2}} \tag{S7}$$

Using the values of $n(\omega)$ and $k(\omega)$, calculate the reflectance $R(\omega)$ of EM waves when they were positive incident on the system using the following formula:

$$R(\omega)=\frac{(n-1)^2+k^2}{(n+1)^2+k^2}=\left(\frac{1-\sqrt{\varepsilon(\omega)}}{1+\sqrt{\varepsilon(\omega)}}\right)^2 \tag{S8}$$

The absorption coefficient $\alpha(\omega)$ of each system can be assessed by the following formula:

$$\alpha(\omega)=\frac{2k(\omega)}{c\mathrm{h}}=\frac{\varepsilon_2(\omega)}{nc\mathrm{h}} \tag{S9}$$

where c represents the speed of light in a vacuum, and h was the unit of energy.

2. Results and Discussion

2.1 Phonon dispersion analysis

We calculated the phonon dispersion curve of the original graphene, which was consistent with the results of previous experimental data[53] and theoretical research[54], as shown in Figure S1. On this basis, we carried out the calculation of phonon dispersion in the TMNG system, and the calculation results are shown in Figure S1 (b). The findings indicate that all frequencies are positive, suggesting that the structure is in a stable state. Therefore, TMNG is considered to be readily synthesizable experimentally.

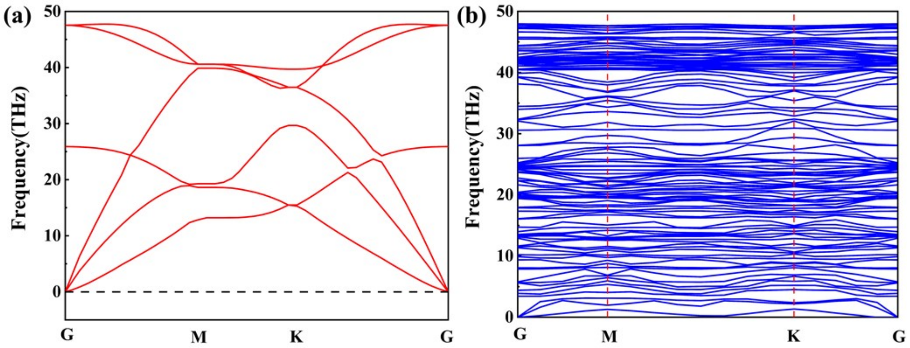

Figure S1. The phonon spectra of (a) monolayer graphene and (b) CoNG are presented

2.2 Band structure

The electronic structures and density of states (DOS) of the N/transition metal co-doped graphene systems were analyzed in this study. To obtain high-precision band structures, sampling was performed along the high-symmetry path G–M–K–G in the irreducible Brillouin zone. The projected density of states (PDOS) plots for each system were obtained using a 12×12×1 k-point mesh centered at the G point. A Gaussian smearing width of 0.02 eV was applied to the energy eigenvalues. All electronic parameter calculations were conducted using a spin-polarized mode.

Firstly, the electronic band structure and DOS of pristine graphene (MG) were calculated, as shown in Figure S2. As illustrated in Figure 1, after optimization, the lattice constant of the 4×4 supercell was determined to be 9.84 Å, and the C–C bond length was 1.42 Å. According to the band structure and total density of states (TDOS) of MG (Figure S2(a)(b)), its valence band maximum (VBM) and conduction band minimum (CBM) (i.e., the π and π^* bands) are located at the high-symmetry K point. Since the CBM and VBM of graphene overlap at the Fermi level, MG exhibits a zero bandgap characteristic and a linear dispersion relation at the K point (i.e., the Dirac point), indicating semi-metallic behavior. This suggests that it is neither a typical metal nor an insulator, but rather a zero-bandgap semiconductor. The electronic band structure and DOS of N-doped graphene are presented in Figure S2(c)(d). Analysis of the band structure and DOS of N-doped graphene (NG) reveals that nitrogen-doped graphene possesses a bandgap of 0.2 eV. Due to the electron-rich nature of nitrogen atoms compared to carbon atoms, the Fermi level in the band structure of this system is significantly shifted above the Dirac point, indicating n-type semiconductor characteristics.

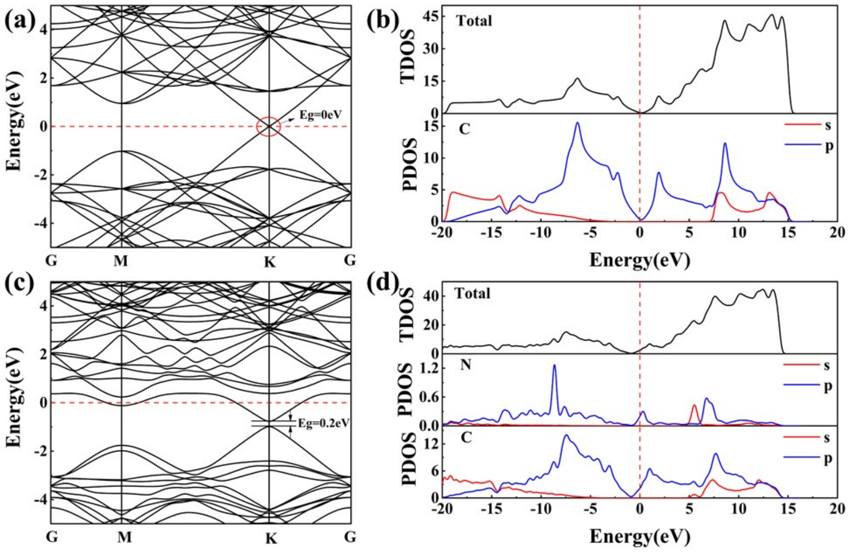

Figure S2. The electronic band structure and density of states of (a)-(b) monolayer graphene and (c)-(d) N-doped graphene are presented

2.3 Density of states

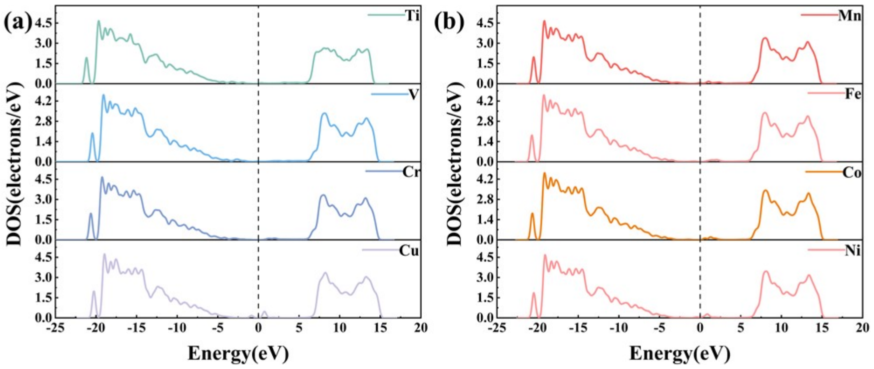

Figure S3. Density of states of C 2s in each doped system

2.4 Charge transfer mechanisms

The results of the TMNG differential charge density calculation are shown in Figure 5 and S4, where blue represents electron-depleted regions and red represents electron-rich regions. The figure indicates that the charge is mainly concentrated near the C-TM and N-TM bonds, and closer to the carbon and nitrogen atoms, suggesting that during the doping process, the carbon and nitrogen atoms gain electrons while the TM atoms lose electrons. Additionally, this study also calculated the Mulliken charge distribution for each system. After co-doping with transition metals and nitrogen atoms, the charges of the individual transition metal atoms are 1.56e, 1.46e, 1.37e, 1.24e, 1.29e, 1.29e, 1.21e, and 1.28e, respectively. The charge transfer of TM atoms in the co-doping system is influenced by N atoms. It is found that as the atomic number increases, the charge of the transition metal atoms decreases (Figure S4). However, for co-doped graphene with strongly magnetic Mn, Fe, Co, and Ni, the change is oscillatory (Figure 5). It is also observed that regions of electron accumulation appear around the transition metal atoms, which is due to their strong interaction with the π electrons of graphene, forming a spin-polarized localized magnetic state (resonant state) with energy near the Fermi level.

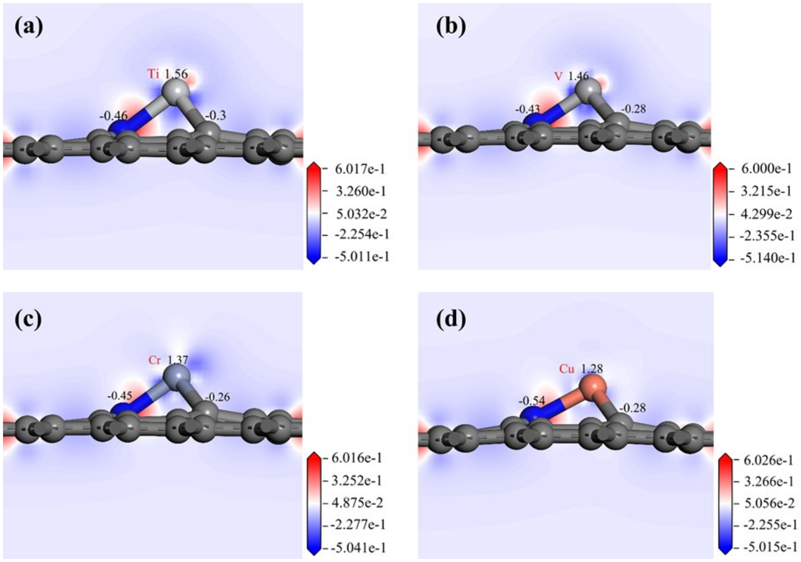

Figure S4. Charge difference density and Mulliken diagrams; (a) Ti; (b) V; (c) Cr; (d) Cu

2.5 CoN_xG System

The calculated binding energies of CoN_xG are shown in Table S1. It is found that the higher the doping N concentration, the lower the absolute value of the binding energy, but the absolute value of the binding energy is the highest under the doping of double vacancies. The result analysis is consistent with the description above. Among them, due to the structure of CoN_3G and CoN_4G, the transition metal is not adjacent to the C atom, while in the CoN_4G system, the Co atom does not protrude from the plane.

Table S1. shows the binding energy (E_b) of CoN_xG, the height h(Å) of Co atoms from the graphene plane, and the optimized bond lengths $l_{C\text{-}Co}$(Å) and $l_{N\text{-}Co}$(Å) after geometric structure optimization.

System	E_b(eV)	h(Å)	$l_{C\text{-}Co}$(Å)	$l_{N\text{-}Co}$(Å)
CoNG	-6.90	1.160	1.782	1.798
CoN_2G	-6.24	1.222	1.773	1.832
CoN_3G	-5.34	1.315	—	1.854
CoN_4G	-8.33	—	—	1.889

Due to the high consumption of phonon spectrum computing resources, the phonon spectra of more representative configurations were selected. The phonon spectra of CoNG were calculated above, and the phonon spectra of CoN_4G were calculated during concentration control, as shown in Figure S5, and all frequencies were found to be positive, indicating that it is also in a stable state.

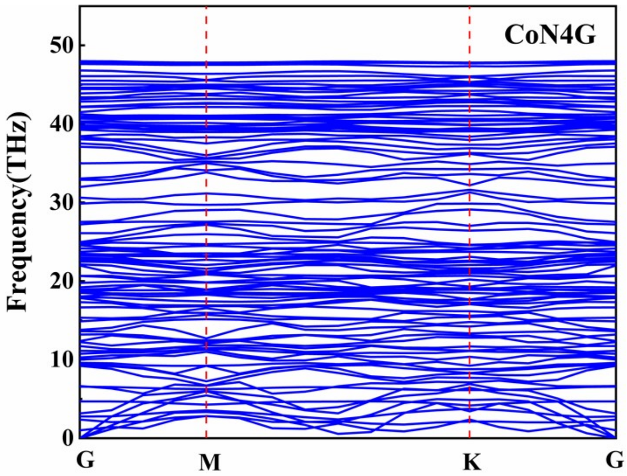

Figure S5. Phonon spectrum of CoN_4G

Figure S6 shows the differential charge density results of the CoN_xG system, which are similar to the TMNG system, with charge transfer slightly affected by the concentration of N atoms.

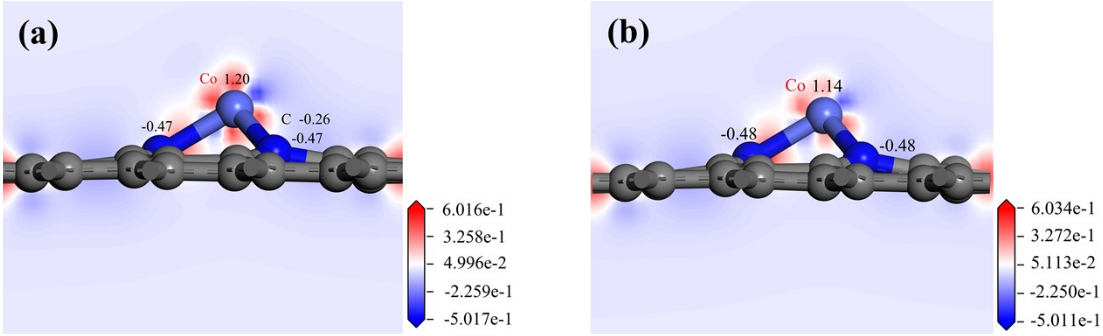

Figure S6. Charge difference density and Mulliken diagrams; (a) CoN_2G, (b) CoN_3G